Measurement of the Global CP Violation in the Decay Mode $B^{\pm} \longrightarrow K^{\pm}\pi^{+}\pi^{-}$

Andreas Mastronikolis
Physics and Astronomy Department, University of Manchester.
(This experiment was performed in collaboration with Flavio Ciciriello)
(Dated: January 28, 2021)

This report summarizes investigations on the global CP violation of the charmless decay modes $B^{\pm} \longmapsto K^{\pm}\pi^{+}\pi^{-}$, isolated from a dataset of $3 \cdot 10^{6}$ events, collected by CERN's LHCb detector in 2011. The said decay mode was found to have a global CP asymmetry of $A_{\mathrm{CP}} = 0.070 \pm 0.022 \pm 0.003 \pm 0.007$, where the first quoted uncertainty is statistical, the second is detector systematic and the last corresponds to the inherent CP violation of the $B^{\pm} \longmapsto J/\psi\,(\mapsto \mu^{+}\mu^{-})\,K^{\pm}$ decay mode. A calculation of the invariant masses of the $B^{\pm}$ and J/ψ mesons was also performed.

I. INTRODUCTION

It is an observational fact that there is a significant imbalance between matter and antimatter in the universe. The earliest theoretical explanation of this experimental fact dates back to a paper published in 1966 by the Soviet physicist Adrei Sakharov, who saw the matter-antimatter disparity as a consequence of three conditions; of which, one required a charge-parity (CP) symmetry violation on the decays of the initial amount of baryons in the Big-Bang [1]. To date, CP violations have been experimentally confirmed multiple times and for different decays [2–4]. This report examines data acquired from the LCHb detector at CERN in 2011 in an attempt to replicate a discovery of a global CP violation in the charmless decay modes:

$$B^{\pm} \longmapsto K^{\pm}\pi^{+}\pi^{-} \tag{I.1}$$

II. APPARATUS

The LHCb apparatus' design is shown in Figure (1). Within the grey tube in the middle of the schematic, two

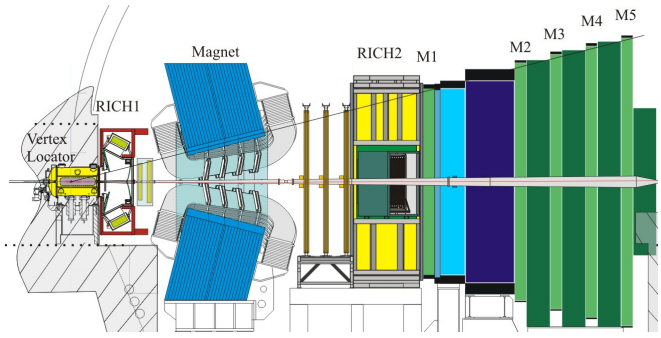

FIG. 1. Detector design of the LHCb with names of different stations. The reader shall bear in mind that some station names were omitted, as information from were not utilized. Courtesy of the LHCb collaboration [5].

beams of protons move in opposite directions until they collide near the vertex locator, which is a detector that surrounds the region where most of the proton−proton (pp) collisions occur and records the first position measurements of the ejected particles. The latter will continue to move with a distribution of momenta rightwards. The RICH1 and RICH2 are *Cherenkov* detectors are dedicated to collect momentum measurements and the muon stations M1−M5 determine whether or not a particle track is formed by a muon [5]. The magnet can operate at two different polarities; up and down. Once a particle enters its region of influence, its trajectory get bent onto different parts of the apparatus. The amount of curvature of such track reveals information about the nature of the particle that forms it and with data collected from the *Cherenkov* detectors, a construction of their initial momentum is attainable.

III. ANALYSIS AND METHODOLOGY

The number of events considered were of the order of 10^{6}. The available data consisted of several vectors with three entries describing values associated with three distinct tracks that were carefully selected to resemble−to a first order of approximation−the decay mode (I.1). The vectors of interest for the forthcoming discussion were the reconstructed momentum vectors of each track along with vectors whose entries are probability measures that dictate whether a particle either a kaon or a pion.

A. Mathematical Formalism

With regards to kinematical analysis, the relativistic framework of four-vectors in the *Minkowski* space was adopted with the metric tensor defined by the convention $\eta^{\mu\nu} = \mathrm{diag}\,(1,-1,-1,-1)$ [6] along with the imposition of natural units; $c = 1$. In this formulation, every particle is represented with a four vector $\tilde{p} = (E, \mathbf{p})$; where E is its energy and $\mathbf{p}$ its 3−dimensional momentum. Via a trivial proof, the invariant mass m of a two-body or a three-body system described sequentially by the four−momenta $\tilde{p_i} = (E_i, \mathbf{p}_i)$ is computed by:

$$m^{2} = \sum_{i=1}^{n} m_i^{2} + \sum_{i=1}^{n}\sum_{j=1}^{n}(1-\delta_{ij})(E_i E_j - \mathbf{p}_i \cdot \mathbf{p}_j) \tag{III.1}$$

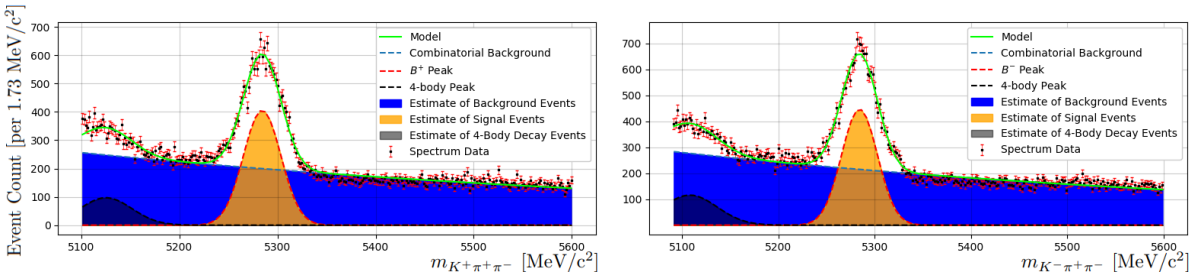

FIG. 2. The best fit of the model (III.2) for the decay modes invariant mass spectra $K^+\pi^+\pi^-$ (left) and $K^-\pi^+\pi^-$ (right) (with the same bin width). The uncertainties shown on the *Spectrum Data* points are the square root of their own value.

where m_i correspond to the invariant mass of the $i-$th particle, δ_{ij} is the Kronecker−Delta and n can be either 2 or 3, respectively. For brevity, the notation $m_{hh'}$ and $m_{hh'h''}$ shall denote the invariant masses of the systems $h'h$ and $hh'h''$, where h, h' and h'' will be specific particles.

B. Particle Identification

From the totality of the observed events, only a small subset of them was of interest for our analysis; for pp collisions can theoretically lead to a plethora of different decay branches, whose particle nature may vary and need not necessarily contain pions and kaons. Thus, a particle identification algorithm was applied to our sample set with the purpose of selecting only the set of events that best describe the modes (I.1). The constraints imposed for each event were: (i) exactly one particle should have a significant probability of being a $K^\pm$ and the other two should have a high probability of being pions, of which one has charge $+e$ and the other $-e$, (ii) charmed contributions are vetoed by rejecting any event that satisfies $1894 \leq m_{K^\pm\pi^\mp}, m_{\pi^+\pi^-} \leq 1894$ MeV/c^2 [2], (iii) all the events that come from the intermediate meson J/ψ are rejected by imposing $3050 \leq m_{\pi\pi} \leq 3150$ MeV/c^2 and lastly, (iv) all events that contain muons are rejected.

C. Invariant Mass Spectra Decomposition

By isolating the best candidate events, the invariant mass spectra can be obtained by use of (III.1). The *Spectrum Data* points in Figure (2) illustrate the said distributions. Not unexpectedly, contributions to the spectra do not necessarily stem from the $B^\pm$ alone. Although a sharp peak is observed around the $B^\pm$ mass, one can observe non-trivial footprints, which stem predominantly from 4−body decay modes of the B meson and background noise that has managed to pass though the identification criteria [7]. That said, there is a need to model each of the said contributions and measure its exact impact. The signal peak can be sufficiently modelled by a normalized *crystal ball* function $\mathcal{C}$ times a constant [8]. As for the background components, the 4−body decay peak that is closest to the $B^\pm$ mass was modelled with a *Gaussian* $\mathcal{G}$ and the combinatorial background with an exponential [2]. Thus, the following ansatz model is suggested:

$$\mathcal{F}^\pm(m;\mathbf{p}) = \underbrace{A_0^\pm e^{-\lambda^\pm m}}_{\text{Combinatorial Background}} + \underbrace{\mathcal{G}^\pm(m;\mathbf{g}^\pm)}_{\text{Closest 4-Body Peak}} + \underbrace{N^\pm \mathcal{C}^\pm(m;\mathbf{q}^\pm)}_{\text{Signal Peak}} \tag{III.2}$$

where $m \equiv m_{K^\pm\pi^+\pi^-}$, $\mathbf{q}^\pm = (\mu^\pm_{\text{sig.}}, \sigma^\pm_{\text{sig.}}, \beta^\pm, n^\pm)$ denotes the parameter vector of $\mathcal{C}$, $\mathbf{q}^\pm = (A^\pm, \mu^\pm, \sigma^\pm)$ is the parameter vector of $\mathcal{G}$ and $\mathbf{p}^\pm$ is vector of all the parameters of the fit; that is, $\mathbf{p} = (A_0^\pm, \lambda^\pm, \mathbf{g}^\pm, \mathbf{q}^\pm)$. The symbols retain their usual meanings. By minimizing the associated χ^2 distribution for this data sample with respect to (III.2), Figure (2) was obtained.

D. Global CP Violation and Corrections

A good metric to quantify a CP violations in the decay modes (I.1) is by introducing the global asymmetry A_{CP}:

$$A_{\text{CP}} = \frac{N^- - N^+}{N^- + N^+},\ \Delta A_{\text{CP}} = \sqrt{\frac{1 - A_{\text{CP}}^2}{N^+ + N^-}} \tag{III.3}$$

where ΔA_{CP} is the statistical uncertainty on A_{CP}. There are two main components in the uncertainties of $N^\pm$; that ultimately affect ΔA_{CP}. One is associated with the counting statistics of said variables, that are *Poisson* distributed and thus the corresponding component is simply $\sqrt{N^\pm}$ [9]. The other one comes from the process of cleaning the signal from background noise and is obtained by the fit model (III.2). There are a several effects that can make A_{CP} deviate from zero but need not stem from a genuine CP asymmetry. One of them comes from an inherent B meson production asymmetry; that is, a significant amount of pp collisions need not necessarily create the same number of B^+ and B^- mesons, which can ultimately alter the values $N^\pm$ in a specific direction. Another comes from the fact that the detector

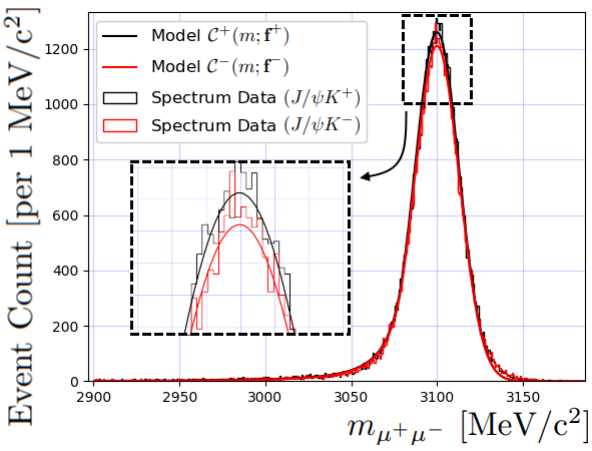

FIG. 3. A plot that illustrates the difference between the number of signal events for the decays $B^\pm \longmapsto J/\psi K^\pm$. The black and red curves represent the fitting model $\mathcal{C}^\pm(m_{\mu^+\mu^-};\mathbf{f}^\pm)$ of the actual data for each case. It is important to note that, in order to isolate the shown data sample, the particle identification criteria changed, as the decay of interest is not (I.1).

might discriminate in detecting positively or negatively charged kaons. To account for the said effects, equation (III.3) is modified by subtracting a correction term $A_{\text{corr.}}$, that measures both production and kaon detection asymmetries. A good estimate for the term was deemed to be the raw asymmetry $B^\pm \longmapsto J/\psi\,(\mapsto \mu^+\mu^-)K^\pm$ corrected by its inherent CP violation term $A_{\text{CP}}(J/\psi K^\pm)$. Thus, $A_{\text{corr.}}$ takes form:

$$A_{\text{corr.}} = \frac{N(J/\psi K^-) - N(J/\psi K^+)}{N(J/\psi K^-) + N(J/\psi K^+)} - A_{\text{CP}}(J/\psi K^\pm)$$

where $N(J/\psi K^\pm)$ denotes the number of signal events for the mode $J/\psi K^\pm$. The quantity $A_{\text{CP}}(J/\psi K^\pm)$ is acquired from work of other researchers and is fixed to the value of 0.001 ± 0.007 [10]. The invariant mass distribution of $\mu^+\mu^-$ was modelled by the crystal-ball functions $\mathcal{C}^\pm(m_{\mu^+\mu^-};\mathbf{f}^\pm)$, where $\mathbf{f}^\pm$ is the parameter vector of the distribution, associated with the decays $B^\pm \longmapsto J/\psi K^\pm$.

IV. RESULTS

After implementing an algorithm that performs the minimization of the χ^2 distribution associated with the considered data sample, the invariant masses that are presented in Table (I) were obtained. By the same reasoning, values of $N^\pm$ were calculated to be $N^+ = 1016 \pm 46$ and $N^- = 1120 \pm 45$. Consequently, the observed CP asymmetry on the (I.1) is 0.049 ± 0.022 and the correction term $A_{\text{corr.}}$ is found to be $-0.021 \pm 0.003 \pm 0.007$. The preceding values yield a global CP asymmetry $A_{\text{CP}} = 0.070 \pm 0.022 \pm 0.003 \pm 0.007$ where the first uncertainty is statistical, the second is associated with systematic errors and the third with the CP asymmetry of the decay $B^\pm \longmapsto J/\psi K^\pm$.

TABLE I. A table that presents the mean values of the invariant mass of the B meson with their associated uncertainties

Particle	Invariant Mass (MeV/c^2)
B^+	5283.70 ± 19.38
B^-	5283.81 ± 19.17
J/ψ [a]	3099.86 ± 12.95
J/ψ	3099.87 ± 12.96

[a] From the $J/\psi K^+$ decay

V. CONCLUSIONS

The global CP asymmetry of the decay mode (I.1) $A_{\text{CP}} = 0.070 \pm 0.022 \pm 0.003 \pm 0.007$ does lie more than three standard deviations away from the the number zero, and thus, evidence for a significant global CP asymmetry is demonstrated. Needless to say, a more precise detector could increase the significance of derived value even further. However, another way such increase might be performed is by executing direct tests to the LHCb apparatus, in order to determine the exact kaon acceptance rates instead of doing it effectively. Lastly, all of the invariant masses summarized in Table (I) are consistent with the accepted values [10]. The dominant source of uncertainty in these results is the precision of the LHCb's apparatus.

[1] D. H. Perkins, *Introduction to High Energy Physics*, 4th ed. (Cambridge University Press, 2014).

[2] R. Aaij and et al., Measurement of CP Violation in the Phase Space of $B^\pm \to K^\pm\pi^-\pi^+$ and $B^\pm \to K^\pm K^- K^+$ Decays, Phys. Rev. Lett. **111** (2013).

[3] A. Alavi-Harati and et al., Observation of Direct CP Violation in $K_{S,L} \longrightarrow \pi\pi$ Decays, Phys. Rev. Lett. **83**, 22–27 (1999).

[4] Measurement of *CP*-violating asymmetries in B^0 decays to *CP* eigenstates, Phys. Rev. Lett. **86**, 2515 (2001).

[5] J. Alves, A.Augusto *et al.* (LHCb), The LHCb Detector at the LHC, JINST **3**, S08005.

[6] N. L. Zakamska, Theory of special relativity (2018), arXiv:1511.02121.

[7] B. Aubert and et al., Evidence for Direct CP Violation from Dalitz−Plot Analysis of $B^\pm \longrightarrow K^\pm\pi^+\pi^-$, Physical Review D **78** (2008).

[8] T. Skwarnicki, *A study of the radiative CASCADE transitions between the Upsilon-Prime and Upsilon resonances*, Ph.D. thesis, Cracow, INP (1986).

[9] R. J. Barlow, *Statistics: A Guide to the Use of Statistical Methods in the Physical Sciences* (Wiley, 1989).

[10] Review of particle physics, Phys. Rev. D **86**, 010001 (2012).